AAZTA-Derived Chelators as Innovative Radiopharmaceuticals

Subjects: Chemistry, Inorganic & Nuclear | Radiology, Nuclear Medicine & Medical Imaging
Contributor: Cyril Fersing

The chelating agent AAZTA features a mesocyclic seven-membered diazepane ring, conferring some of the properties of both acyclic and macrocyclic chelating agents. Described in the early 2000s, AAZTA and its derivatives exhibited interesting properties once complexed with metals and radiometals, combining a fast kinetic of formation with a slow kinetic of dissociation. Importantly, the extremely short coordination reaction times allowed by AAZTA derivatives were particularly suitable for short half-life radioelements (i.e., 68Ga).

Keywords: AAZTA ; bifunctional chelator ; radiopharmaceuticals ; theranostics ; nuclear medicine

1. Introduction

As an emerging approach in modern medicine, “theranostics” (also called “theragnostics”) consists of the combination of diagnostic and therapeutic tools to achieve personalized patient care [1]. Various scientific disciplines, especially in the field of nanotechnology [2] and biomaterials [3], can be involved in theranostic approaches. Nuclear medicine is particularly suited to this concept, easily combining molecular imaging and targeted radionuclide therapy [4]. Historically, nuclear medicine is deeply connected to theranostics, being used for decades for the management of benign and malignant thyroid diseases with radioiodine isotopes [5][6]. In recent years, theranostic in nuclear medicine benefited from the rise of ^{68}Ga and ^{177}Lu radiochemistry, allowing easy radiolabeling of the same vector molecule by either a photon-emitting (i.e., ^{68}Ga for PET imaging) or a particle-emitting (i.e., ^{177}Lu, beta-emitter for therapy) radioelement. This approach is all the more convenient since the radioelements used are metals, which can be readily complexed by a vector molecule functionalized by a chelating group. The “theranostic pair” ^{68}Ga/^{177}Lu is an illustrative example, successfully applied to the management of several malignancies, in particular neuroendocrine tumors (NETs) [7] and prostate cancer [8][9]. New theranostic pairs have recently become increasingly popular, especially those involving scandium-44. This latter positron-emitting isotope showed high potential for TEP imaging and can be paired with either ^{177}Lu or its beta-emitter isotope ^{47}Sc for therapeutic applications [10]. Radiolabeling with radiometals requires optimal coordination chemistry conditions, including the use of chelating groups best suited to the theranostic couples used in nuclear medicine. The complexation reaction step can be industrialized for radioelements with a long half-life (i.e., ^{177}Lu), whereas radiopharmaceuticals containing short half-life radioelements (i.e., ^{68}Ga) have to be prepared extemporaneously, in the radiopharmacy laboratory, under reaction conditions that should be as simple and robust as possible. To date, the chelators of choice for the design of radiopharmaceuticals are either macrocycles such as DOTA (used in DOTATOC, DOTATATE, or PSMA-617) or acyclic groups such as DTPA (used in pentetreotide). However, many new chelating agents with more sophisticated structures and enhanced properties have been developed in recent years [11]. Among these original derivatives, AAZTA (6-amino-6-methylperhydro-1,4-diazepinetetraacetic acid) is a heptadentate chelator formed by a medium-sized, seven-membered 1,4-diazepine ring and an iminodiacetic exocyclic group. This particular structure makes it part of the mesocyclic chelating agents class. The first of these chelators, AAZTA, was initially designed to form gadolinium complexes of particular interest in MRI imaging. In addition to forming a stable complex, Gd-AAZTA could bind with two water molecules in its coordination sphere (hydration number q = 2), reaching high relaxivities. Other chelators inspired by AAZTA were then developed and displayed promising coordination properties for some radiometals such as gallium-68 or scandium-44. Although AAZTA and its derivatives have been thoroughly studied for their possible applications in magnetic resonance imaging (MRI), the use of these chelators for radiochemical applications has only become widespread in recent years.

2. Design, Synthesis, and Kinetic Properties

2.1. Original AAZTA Derivatives

The first synthesis of AAZTA was reported by Aime et al. in 2004, presenting this chelator as a promising MRI contrast agent candidate [12]. The first step of its synthesis sequence (Scheme 1) consisted of the formation of the diazepane ring via a nitro-Mannich reaction. Heating a mixture of *N,N′*-dibenzylethylenediamine diacetate, nitroethane, and formaldehyde in ethanol allowed the formation of 1,4-dibenzyl-6-methyl-6-nitroperhydro-1,4-diazepine in excellent yields. Subsequent reduction of the nitro group and simultaneous bis-*N*-debenzylation catalyzed by palladium on carbon in a methanol/water mixture under hydrogen atmosphere led to 6-amino-6-methylperhydro-1,4-diazepine (AMPED), a strongly basic triamine whose nitrogen atoms can be functionalized. Complete alkylation of both the primary amine and the two secondary amines using *tert*-butylbromoacetate with potassium carbonate in acetonitrile formed the final protected derivative, subsequently treated by trifluoroacetic acid to obtain the AAZTA chelator with a 48% overall yield. In addition to being simple and straightforward, this synthesis has the advantage of using readily available and cheap reactants.

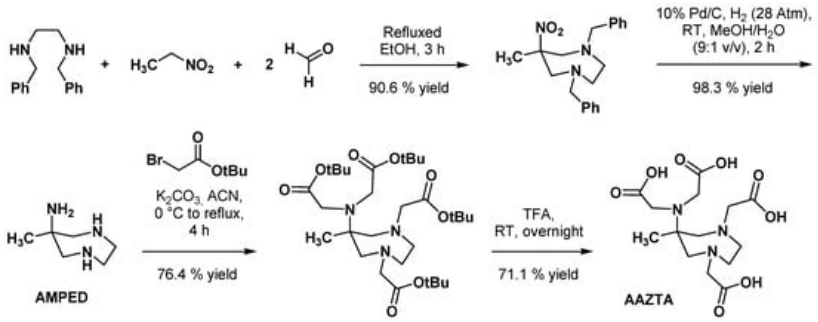

Scheme 1. Original synthesis sequence of AAZTA described by Aime et al. [12].

Evaluated for its potentiometric and relaxometric properties, the $[Gd\text{-}AAZTA]^-$ complex showed a stability constant (log*K*) of 19.26, slightly smaller than $[Gd\text{-}DTPA]^{2-}$. However, this complex displayed no transmetallation effects in the presence of Zn, Mn, or Ca, an exchange rate of the two coordinated water molecules significantly higher than $[Gd\text{-}DTPA]^{2-}$ and $[Gd\text{-}DOTA]^-$ (90 ns vs. 300 ns and 240 ns, respectively) and a high kinetic inertness (unchanged relaxivity at 20 MHz and 298 K for a pH range from 2 to 11). Coordination behavior of AAZTA with other lanthanoids was very comparable, with a monotonous increase in the complexes' stability from La^{3+} to Lu^{3+} but with log*K* values slightly lower than those of the analogous DTPA complexes [13]. Complementary studies confirmed the excellent kinetic inertness of the $[Gd\text{-}AAZTA]^-$ complex near physiological conditions ($t_{1/2}$ = 4337 h vs. 147 h for $[Gd\text{-}DTPA]^{2-}$).

Overall, these results suggested AAZTA compatibility with Ga, Sc, and Lu and the possibility of a safe in vivo use of potential AAZTA-radiopharmaceuticals, especially for the labelling of heat-sensitive biomolecules such as antibodies. The interest of chelators allowing fast complexation at room temperature is major in the design of new radiopharmaceuticals. The best example is HBED, a phenol-containing aliphatic chelator able to form stable complexes with ^{68}Ga at room temperature within minutes [14][15] and found in PSMA-11, widely used in clinics for prostate cancer PET imaging [16].

2.2. AAZTA Modulations to Improve Coordination Behavior

2.2.1. Modifications in the Number and Nature of Coordinating Side Arms

Replacement of the two acetic arms in the 1,4 position of AAZTA by bulkier methyleneethylphosphinic groups was reported by Emerlindo et al. in 2013 [17]. Because the Mannich reaction between AMPED, paraformaldehyde, and alkylphosphinate ester quantitatively formed a tricyclic bisaminal derivative in place of the expected product, the phosphinic pendant arms were introduced first, in the form of a methanesulfonic acid ethoxymethylphosphinyl ethyl ester. Alkylation of AMPED with this latter occurred preferentially at endocyclic nitrogen atoms (Scheme 2), most certainly due to both high steric hindrance at the 6-amino position and high nucleophilicity of the secondary amines [13][18]. *N*,*N*-Dialkylation of the 6-amino position with *ter*-butyl bromoacetate was conducted afterward to obtain, after deprotection by hydrobromic acid, the $AAZ2A2P^{Et}$ chelator in 7% overall yields. The [Gd- $AAZ2A2P^{Et}$] complex was characterized by a coordination environment very similar to [Gd-AAZTA], except for its reduced number of coordinated water molecules (*q* = 1, possibly due to the steric hindrance of the phosphinate groups). Most importantly, this work showed the possibility of starting from AMPED as a scaffold for chelating arms' modulation.

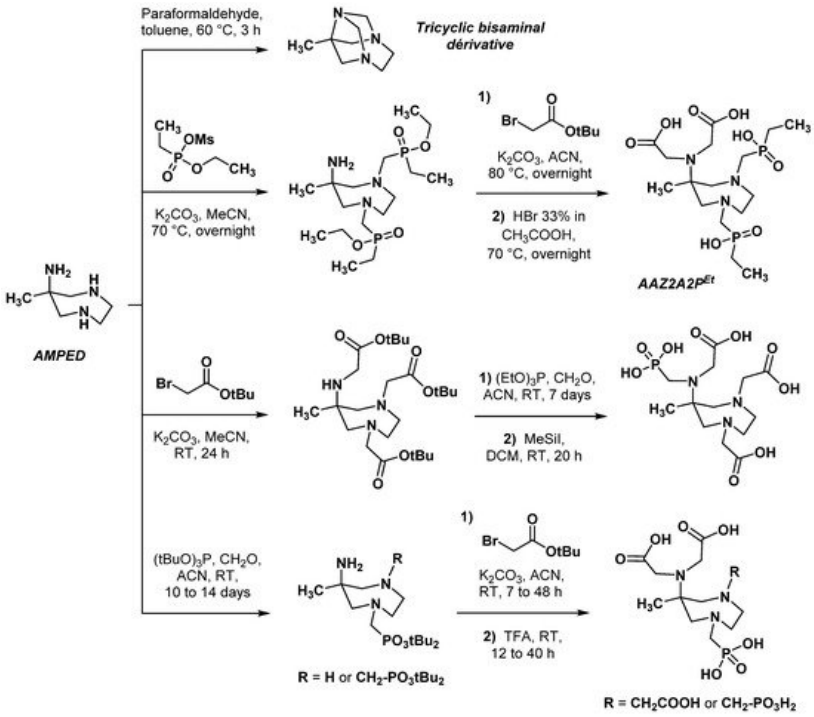

Scheme 2. Synthesis sequence of phosphorus-containing AAZTA derivatives described by Ermelindo et al. [17] and Guanci et al. [19]. Ms = methanesulfonate.

AAZTA derivatives bearing a glutar-2-yl group at one or both endocyclic nitrogen atoms were synthesized by Elemento et al. [18]. Selective alkylation relied on the preferential reactivity of the secondary amines and gave rise to several diastereoisomers (**Figure 1**). Water exchange rates measured for Gd^{III} complexes of mono- and di-glutarate derivatives were slightly lower than for Gd-AAZTA, with a metal ion hydration number $q \approx 2$ for each complex. Interestingly, faster exchange dynamics were observed for the (*RS*) derivative compared to its (*RR*) diastereoisomer, suggesting that small modulations on the diazepane ring substituents could increase the steric demand at the metal center. Evaluation of such chelators as radiometal complexing agents would be relevant, especially with regard to the free carboxylate groups on the glutarate arms that could offer the possibility for conjugation reactions.

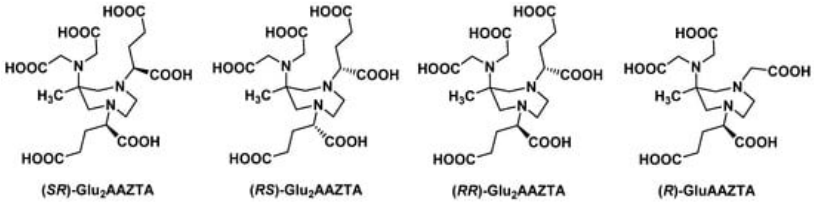

Figure 1. Examples of mono- and di-glutarate analogues of AAZTA synthesized by Elemento et al. [18].

2.2.2. Backbone Rigidification

Structure rigidification by fusing a cyclic unit to the backbone of a chelating agent is a strategy that has already been applied to acyclic ligands such as DTPA. The cyclohexyl ring of CHX-A″-DTPA made the complexing agent stiffer, imposing a degree of preorganization on the metal ion binding site and enhancing its kinetic inertness [20][21]. With the same goal, a cyclohexyl-fused AAZTA chelator (CyAAZTA) was synthesized and studied [22]. CyAAZTA was obtained following a synthesis sequence analogous to AAZTA, starting from *trans*-1,2-dibenzylaminocyclohexane (Scheme 3).

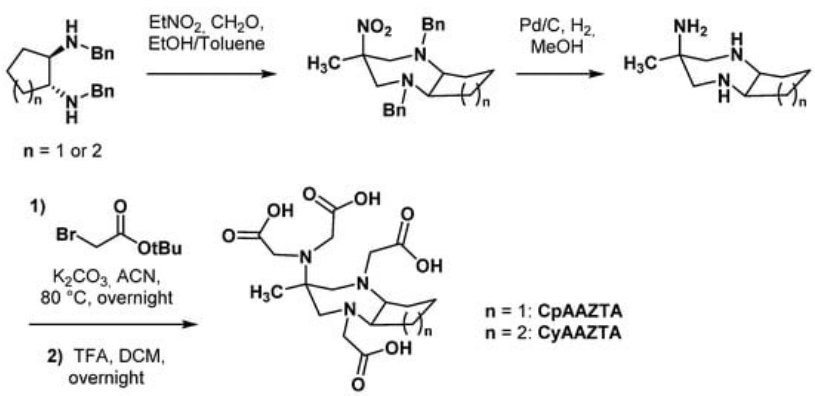

Scheme 3. Synthesis of constrained chelators CyAAZTA [22] and CpAAZTA [23].

A cyclopentyl-fused analogue of CyAAZTA, called CpAAZTA, was also reported [23]. Its synthesis was comparable in every way with that of CyAAZTA, starting from 1,2-epoxycyclopentane as the precursor of *trans*-1,2-dibenzylaminocyclopentane (Scheme 3).

2.3. AAZTA Modulations to Obtain Bifunctional Chelating Agents (BCA)

Various techniques for anchoring a chelating agent to a molecule of interest are described in the literature, each of them requiring the presence of a dedicated reactive group on the chelator to undergo this functionalization [24][25]. In the AAZTA structure, the methyl group on the sp^3 central carbon atom of the propylene endocyclic moiety is particularly suitable for derivatization as it is exocyclic and not involved in metal ion complexation. Hence, several methyl-modified analogues were designed for their further bioconjugation. Hydroxymethyl AAZTA derivative (AAZTA-MeOH) was described by Sengar et al. and was synthesized following a procedure similar to the original reaction sequence (Scheme 4), nitroethane being replaced with 2-nitroethanol [26]. However, the last deprotection step with trifluoroacetic acid (TFA) led to the formation of a lactone after cyclization between the hydroxyl group with one of the two *tert*-butyl esters located on the exocyclic nitrogen. This unwanted esterification called for an additional basic hydrolysis step prior to the coordination reaction. Interestingly, no such lactonization was observed during the synthesis of the hydroxyethyl AAZTA derivative (AAZTA-EtOH) (Scheme 4), the seven-ring formation being less favorable than the six-ring one. Crystal structures of Gd^{III} and Eu^{III} complexes of AAZTA-MeOH and AAZTA-EtOH showed no direct participation of the hydroxyl side chain in the metal ion chelation, which confirmed this position as an adequate functionalization site.

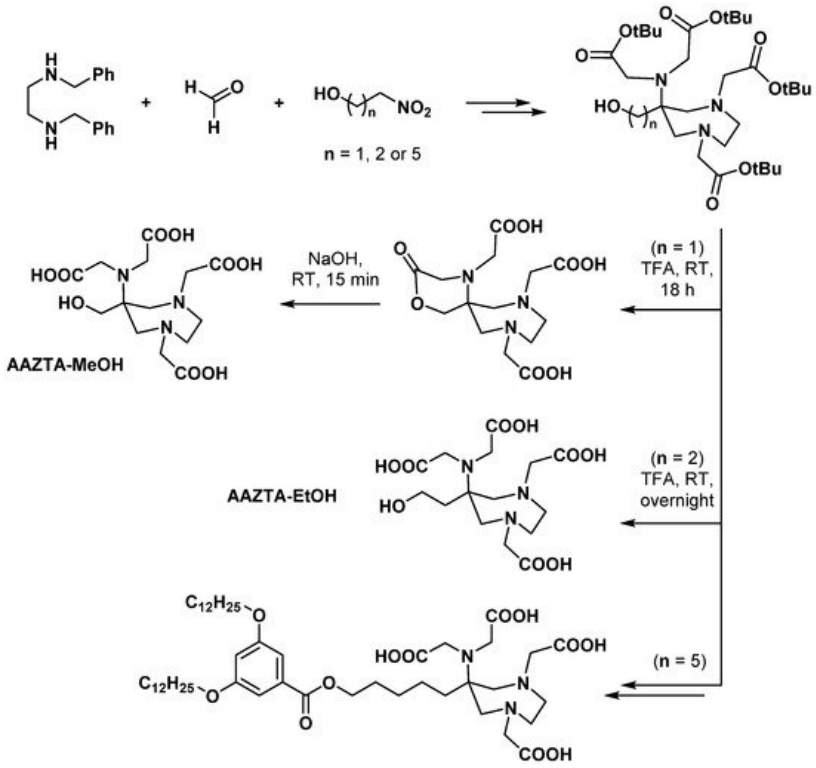

Scheme 4. Synthesis of hydroxyalkyl AAZTA derivatives as BCA [26][27].

2.4. AAZ3A Derivatives

Six-coordinate Ga^{III} complexes are known to reach excellent stability [28], the metal environment forming a more or less distorted octahedral geometry as with Ga-DOTA complexes. To design new hexadentate AAZTA-derived chelators, Parker et al. synthesized several derivatives characterized by an “N3O3” donor set and a single acetate arm on the 6-amino group [29]. These derivatives will be later named DATA chelators after their 6-amino-1,4-diazepine triacetate scaffold. Some of these analogues also incorporated a bulkier 6-phenyl moiety instead of the 6-methyl moiety of AAZTA, so that the 6-amino group is most likely to adopt an axial position that would form a facing-capping array with the three nitrogen atoms. However, this substitution modified the stability of the diazepane ring in such a way that subsequent hydrogenolysis using Pd/C caused ring opening. Acid-labile 2,4-dimethoxybenzyl groups were then used to protect cyclic amines. After deprotection by TFA and alkylation of the two endocyclic nitrogen atoms (Scheme 5), reduction of the nitro group was then achieved with Raney nickel in ethanol at RT. Finally, selective mono-alkylation of the resulting primary

amine has been achieved using the appropriate α-bromo ester. Some derivatives also underwent a *N*-methylation reaction of the 6-amino group, using iodomethane in acetonitrile.

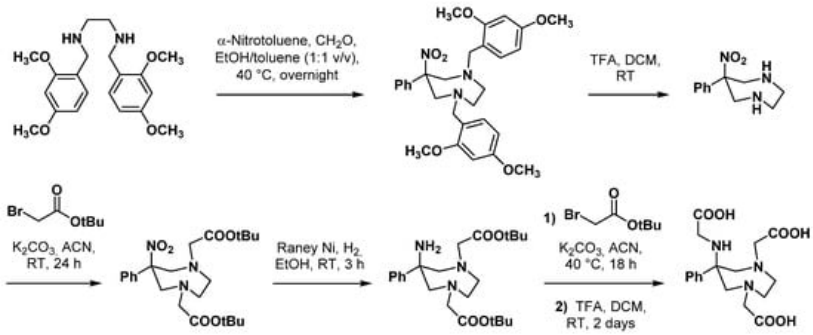

Scheme 5. Synthesis of 6-amino-1,4-diazepine triacetate chelating agents [29].

3. Applications in Nuclear Medicine

Despite the undeniable kinetic improvements brought by DATA derivatives over AAZTA, this latter chelating agent was the most exemplified mesocyclic-complex-forming unit in innovative PET imaging probes. This could be explained by the more straightforward synthesis sequence of AAZTA, which is easier to deploy in proof-of-concept works. Several types of vectors, such as peptides, small molecules, or even monoclonal antibodies, have been used as substrates for bioconjugation with AAZTA-derived bifunctional agents.

3.1. Monoclonal Antibodies

Bifunctional chelating agents compatible with mild radiolabeling reaction conditions are particularly needed for monoclonal antibodies (mAbs) functionalization, as mAbs are heat- and pH-sensitive macromolecules. In this view, Klasen et al. combined an AAZTA^5 scaffold with a squaramide ester motive and coupled this BCA to a model antibody (bevacizumab) [30]. This ligation technique, based on the pH-dependent reactivity of squaric acid diethyl ester, is increasingly used in the design of new radiopharmaceuticals [31]. Starting from protected AAZTA^5, methyl ester could be selectively hydrolyzed with lithium hydroxide and the resulting carboxylic acid further coupled with *N*-Boc-ethylenediamine. After deprotection of both *tert*-butyl-ester- and Boc-protecting groups, the resulting compound was immediately coupled with squaric acid (SA) diethyl ester. Finally, bioconjugation with bevacizumab was conducted in mild conditions (Scheme 6).

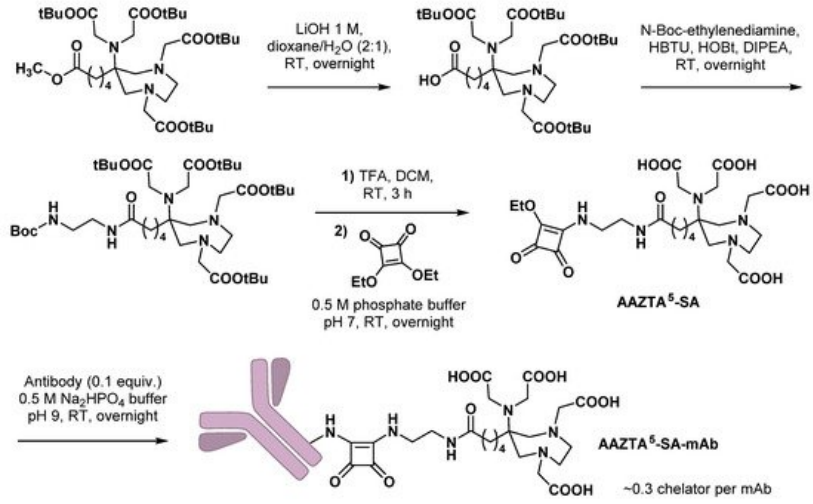

Scheme 6. Synthesis of AAZTA^5-SA bifunctional agent and bioconjugation reaction with a mAb, as reported by Klasen et al. [30].

3.2. Small Molecules

3.2.1. Dual MRI/PET Imaging Agents

One of the earliest PET imaging applications involving an AAZTA chelator was reported by Vologdin et al. and consisted of a heterodimeric DO3A-sulfonamide-AAZTA ligand presented as a potential pH-sensitive dual MRI/PET probe [32]. The pH-responsiveness of this molecule was due to the sulfonamide nitrogen that changed the hydration state of the Gd complexed with DO3A at pH > 8 [33], without interacting with the adjacent [^{68}Ga]Ga-AAZTA complex. The main issue in the

synthesis of this Gd-Ga heterobimetallic complex was the need for two different orthogonal protecting groups for the carboxylic acids of each chelator, DO3A and AAZTA, allowing sequential and selective complexations (Scheme 7).

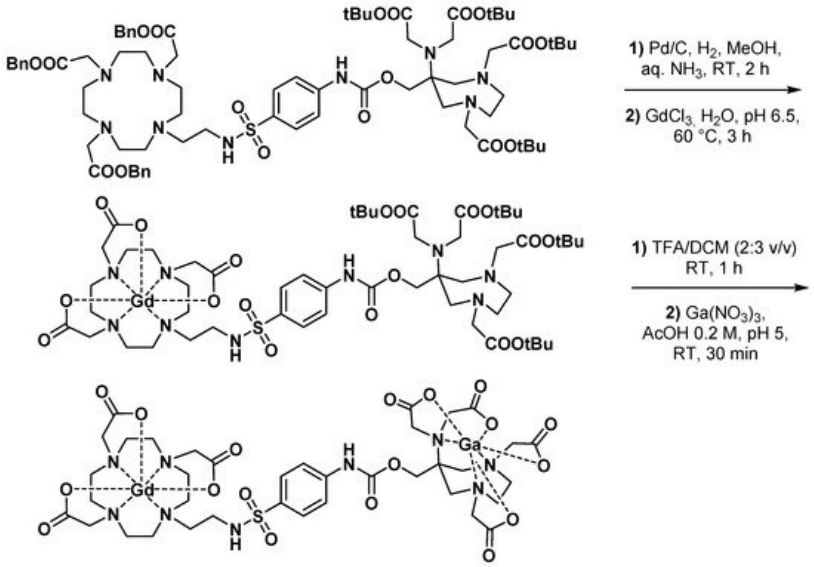

Scheme 7. Synthesis and labeling of the DO3A-sulfonamide-AAZTA pH-sensitive described by Vologdin et al. [32].

3.2.2. Bisphosphonate Derivatives

Starting from AAZTA-MeOH, Wu et al. designed a phenoxy-containing BCA (PhenA) that was coupled to bisphosphonate derivatives [34]. These compounds were then radiolabeled with ^{68}Ga and evaluated as bone PET imaging agents. PhenA could be obtained through a high-yield five-step synthesis (Scheme 8).

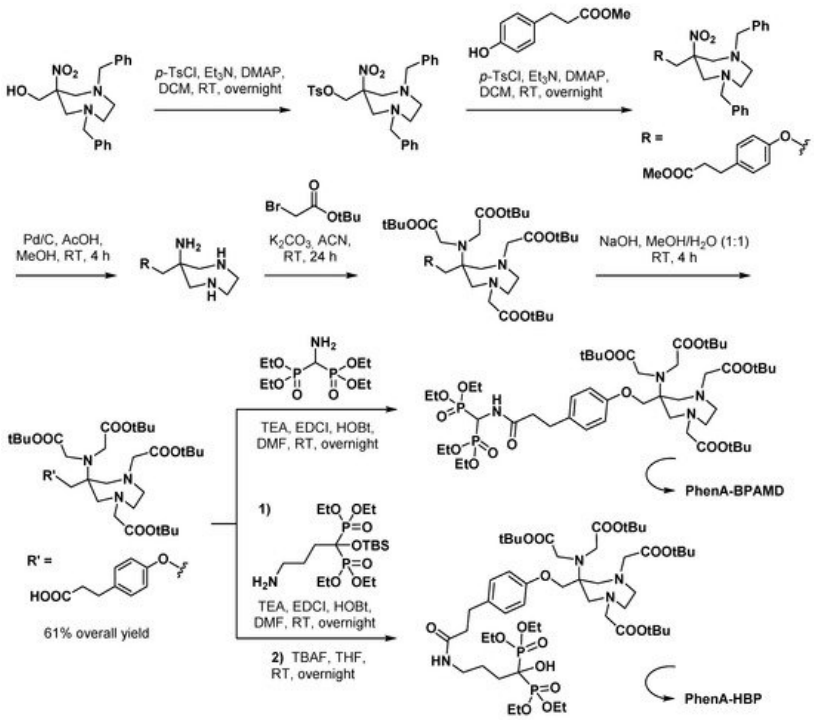

Scheme 8. Synthesis of bisphosphonate-containing PET imaging agent candidates reported by Wu et al. [34].

3.2.3. Curcumin Derivatives

To expand the potential applications of curcumin derivatives to nuclear medicine imaging of cancers, Orteca et al. developed new targeting vectors based on curcumin scaffolds functionalized with AAZTA or NODAGA chelators [35]. Synthesis of NODAGA-C21 and AAZTA-PC21 was performed in four and five steps, respectively, with pyrazole derivatization of the curcumin keto-enol moiety in the preparation sequence of AAZTA-PC21. A protected pentanoic acid AAZTA derivative (AAZTA^5) was used as a bifonctionnal agent and was conveniently coupled with the pyrazine curcumin derivative via amide bond formation (Scheme 9).

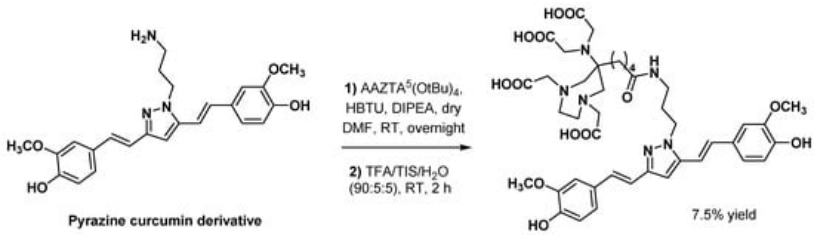

Scheme 9. Conjugation of protected AAZTA^5 chelator with a pyrazine curcumin derivative, as described by Orteca et al. [35].

3.2.4. Prostate-Specific Antigen Ligands

Sinnes et al. explored the influence of the chelator part on the in vitro characteristics of a PSMA vector molecule by replacing DOTA with AAZTA^5 in PSMA-617 [36]. The resulting AAZTA^5-PSMA-617 (**Figure 2**) was successfully radiolabeled with ^{68}Ga, ^{44}Sc, and ^{177}Lu at RT within 5 min, reaching >99% RCY for a chelator-to-radiometal molar ratio = 10:1. Both [^{68}Ga]Ga- and [^{44}Sc]Sc-AAZTA^5-PSMA-617 were extremely stable in human serum, PBS, and EDTA/DTPA in PBS (>90% RCP over 2 h for the ^{68}Ga derivative and >95% RCP over 8 h for the ^{44}Sc derivative).

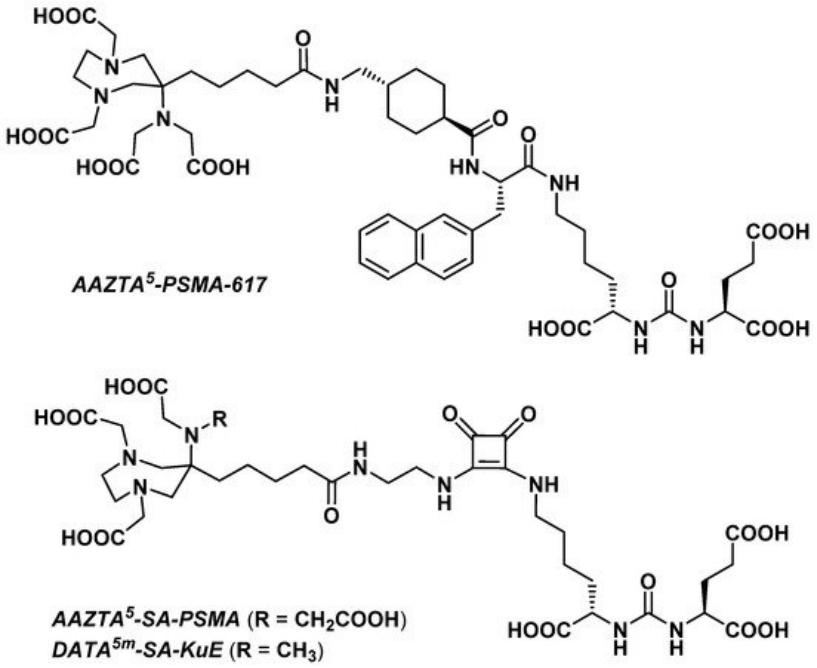

Figure 2. Structure of PSMA ligands functionalized with AAZTA-derived chelator.

The [^{44}Sc]Sc-AAZTA^5-PSMA-617 derivative was later evaluated in vivo after an in-depth study of the radiolabeling reaction conditions [37]. Although its amount in radiopharmaceuticals is strictly limited by European Pharmacopoeia [38], HEPES 0.1 M was found to be a particularly suitable buffer to reach high RCY and excellent molar activity (average of 39.4 GBq/µmol) at pH 4. To achieve quantitative RCY at neutral pH, a higher peptide concentration (10 µM rather than 1 µM) was necessary. [^{44}Sc]Sc-AAZTA^5-PSMA-617 confirmed its stability in human plasma over 24 h, and in vitro cellular uptake studies showed a higher accumulation of AAZTA-containing radioligands in LNCaP cells compared to their DOTA-containing analogues. Preclinical PET imaging and ex vivo biodistribution studies with [^{68}Ga]Ga- and [^{44}Sc]Sc-AAZTA^5-PSMA-617 in LNCaP tumor-bearing mice concluded a higher accumulation of the [^{44}Sc]Sc-AAZTA derivative in tumors than its DOTA analogue (14.98 vs. 7.49 %ID/g, 3 h post-injection), possibly due to a two times higher molar activity. Self-blocking experiments confirmed the PSMA specificity of these radioligands. Overall, the good radiolabeling characteristics and intrinsic physicochemical properties of [^{44}Sc]Sc-AAZTA^5-PSMA-617 allowed its good in vivo imaging performance on a xenografted mouse model versus one of the most relevant PSMA derivatives used in clinics, i.e., DOTA-PSMA-617, confirming the potential of this AAZTA-conjugate for clinical translation.

3.2.5. Fibroblast Activation Protein Inhibitors

Fibroblast activation protein α (FAP) is an endopeptidase that is found upregulated in various tumor types. It is an important marker of cancer-associated fibroblasts that appears to contribute to some of their tumor-promoting activities [39]. After the identification of the FAP inhibitor (FAPi) lead molecule UAMC-1110 [40], many FAP-targeting imaging tools based on the same quinoline scaffold were designed for theranostic applications in a variety of cancers [41][42]. For that purpose, the use of the squaramide motif to anchor a chelating moiety on a vector molecule has been exemplified with

FAPi compounds: the team of Frank Rösch synthesized and evaluated a DATA^{5m}-SA-FAPi derivative in comparison with its DOTA analogue [43]. Starting from the quinoline NH_2-UAMC-1110, both DOTA and DATA^{5m}-bearing molecules were obtained following a convenient preparation procedure that relied on the simple coupling conditions allowed by the pH-dependent reactivity of SA (Scheme 10).

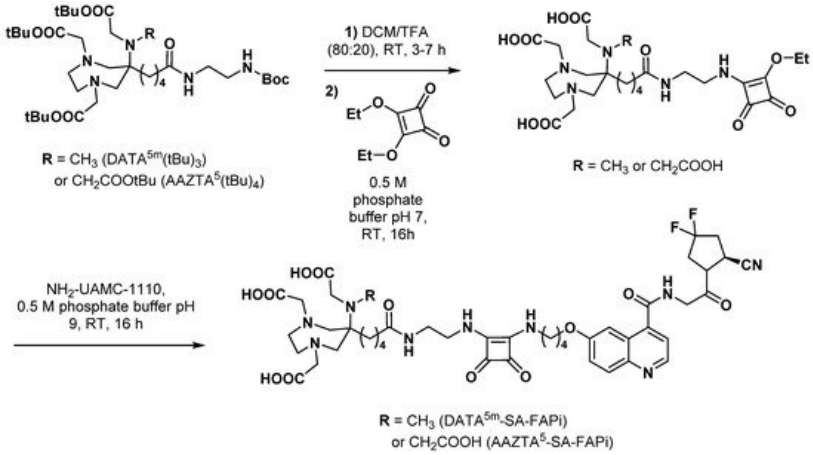

Scheme 10. Synthesis of AAZTA^5- and DATA^{5m}-SA-FAPi derivatives [43][44].

3.3. Peptides

Due to their reasonable convenience of synthesis, adapted pharmacokinetic behavior, and high target specificity, peptide probes are widely exploited in the conception of theranostic agents in nuclear medicine. The first radiolabeled peptide used in humans was the somatostatin analogue [^{123}I]I-204-090 developed in 1989 [45], which paved the way to [^{111}In]In-DTPA-Octreotide [46] and several other DOTA-containing somatostatin analogues [47][48][49]. In addition to the search for various new targets, novel complexing agents such as AAZTA are being evaluated to allow easy and rapid radiolabeling of these peptide vectors with radiometals.

3.3.1. RGD Peptides

Functionalization of a peptide with AAZTA^5 was first described by Manzoni et al. [50], who prepared about ten RGD peptidomimetic conjugates bearing different chelating groups. Modified integrin $\alpha_V\beta_3$ ligand DB58, incorporating an azide group, was chosen for functionalization. After hydrogenation with Pd/C to get the corresponding amine, it was coupled to either AAZTA^5(OtBu)$_4$ or its spacer-containing analogue, using standard amide bond formation procedures (Scheme 11).

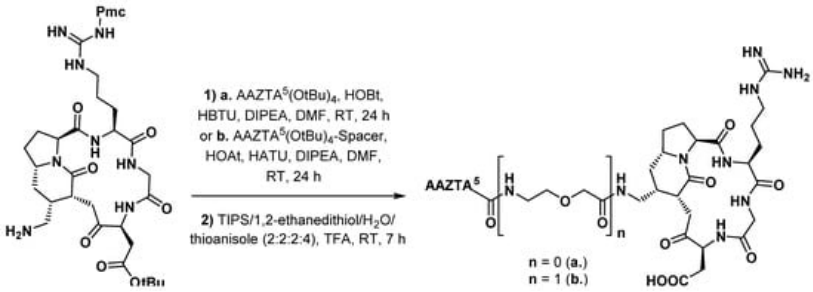

Scheme 11. Functionalization of the RGD peptidomimetic DB58 with AAZTA chelating agents, as proposed by Manzoni et al. [50].

3.3.2. Gastrin Analogues

Cholecystokinin 2 receptor (CCK2r), which is overexpressed in various tumor tissues (e.g., medullary thyroid carcinoma [51] or gastrointestinal stromal tumors [52]), can be targeted with gastrin analogues [53]. In this light, Pfister et al. designed an AAZTA-containing gastrin (10–17) (minigastrin, MG) analogue as an original theranostic tool targeting CCK2r (**Figure 3**) [54].

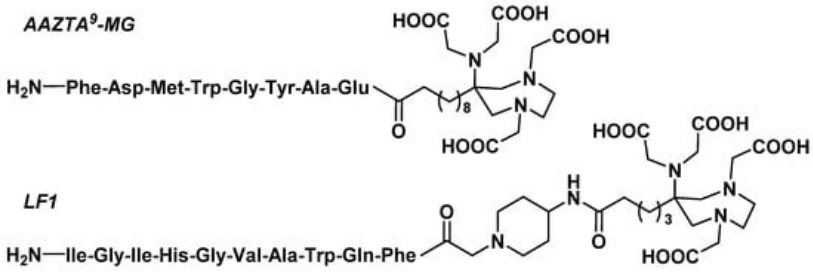

Figure 3. Structure of AAZTA^{9}-MG and LF1.

3.3.3. Octreotide Analogues

Somatostatin receptor (sstr) ligand analogues are the most well-developed and extensively investigated group of small peptides functionalized by a chelating agent [55]. Since the regulatory approval of [^{111}In]In-DTPA^{0}-octreotide for scintigraphic imaging of sstr expression [56], modulations were conducted both on the peptide and on the chelator part of these imaging agents to optimize their selectivity, receptor binding affinity, internalization, pharmacokinetic properties, or radiolabeling abilities.

To evaluate the properties of a mesocyclic ligand on this type of targeting vector, AAZTA^{5}-TOC was synthesized via a simple peptide coupling between AAZTA^{5} and Phe^{1}-Tyr^{3}-octreotide (TOC) [57]. Radiolabeling with ^{68}Ga, ^{44}Sc, and ^{177}Lu reached high RCY after 1 min reaction time at RT with optimized precursor amounts (10 nmol for ^{68}Ga and ^{44}Sc assays; 1:10 lutetium-to-precursor molar ratio for ^{177}Lu assay). Interestingly, pH variations in the 4.5–5.5 range had no influence on labeling speed or yields. Concerning in vitro stability, only [^{68}Ga]Ga-AAZTA^{5}-TOC showed slight instability (85% RCP) and sensitivity to transchelation (40–50% RCP) in human serum after 2 h. Despite the promising preliminary results of AAZTA^{5}-TOC, its development has not yet reached clinics. In contrast, its analogue, DATA^{5m}-TOC, described 2 years before, attained the clinical development stage. Initial work by Seeman et al. on this PET tracer candidate consisted of elaborating a kit-type labeling protocol at RT [58]. A two-step sequence very similar to AAZTA^{5}-TOC afforded DATA^{5m}-TOC in 31% yield (Scheme 12). Then, ^{68}Ga radiolabeling assays were carried out using four different eluate post-processing methods. Remarkably, >95% RCYs were achieved within 1 min at pH 4.9 and RT with fractionated and acetone post-processing. Peptide concentration, slightly higher in these two conditions, may also have an influence on these results. Regardless of the post-processing method, >98% RCYs were reached within 10 min in each case.

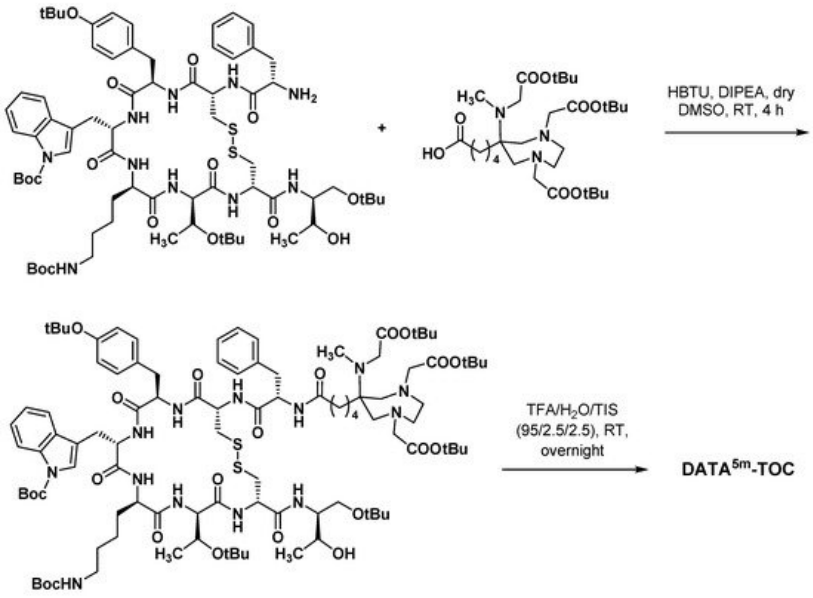

Scheme 12. Synthesis of DATA^{5m}-TOC according to Seeman et al. [58].

4. Conclusions

Since its early patenting [59], AAZTA has positioned itself as a promising chelating agent for imaging applications, opening the way to a family of compounds halfway between the well-known linear and macrocyclic chelating agents. The design and fairly convenient synthesis of various analogues of AAZTA allowed us to investigate their kinetic and thermodynamic properties with several metal ions. However, only AAZTA and DATA^{5m} were used in the development of original vector molecules for nuclear medicine applications. Their reactivity at room temperature and their compatibility with a wide pH range may pave the way for the design of theranostic agents based on pH- or heat-sensitive biomolecules. Regarding the

conception and evaluation of new AAZTA-containing probes, works highlighted the need for a systematic validation approach, with careful in vitro measurement of physicochemical parameters, stability, and affinity of the AZZTA-conjugate with its target. These results should be confirmed with in vivo biodistribution studies and microPET imaging on relevant animal models, possibly with several radioelements in a theranostic perspective. Only a few AAZTA-containing molecules have yet been evaluated in patients for imaging applications. It is reasonable to think that the therapeutic applications of these same vectors will take even longer to be evaluated in humans, considering the complexity for therapeutic radiopharmaceuticals to reach clinical evaluation stages. During the radiolabeling step, a significant portion of the final RCY can be achieved within minutes, making AAZTA particularly suitable for short half-life radioelements such as ^{68}Ga. With shorter preparation times, higher batch activities, and possible cost-effective single vial cold kit formulation, the use of AAZTA-derived chelators could facilitate the clinical transfer of vector candidates and encourage even more the expansion of theranostic approaches in nuclear medicine.

References

1. Kelkar, S.S.; Reineke, T.M. Theranostics: Combining imaging and therapy. Bioconjug. Chem. 2011, 22, 1879–1903.
2. Cai, Y.; Chen, X.; Si, J.; Mou, X.; Dong, X. All-in-one nanomedicine: Multifunctional single-component nanoparticles for cancer theranostics. Small 2021, 17, 2103072.
3. Kharbikar, B.N.; Zhong, J.X.; Cuylear, D.L.; Perez, C.A.; Desai, T.A. Theranostic biomaterials for tissue engineering. Curr. Opin. Biomed. Eng. 2021, 19, 100299.
4. Langbein, T.; Weber, W.A.; Eiber, M. Future of theranostics: An outlook on precision oncology in Nuclear Medicine. J. Nucl. Med. 2019, 60, 13S–19S.
5. Hertz, S. Radioactive iodine in the study of thyroid physiology: VII. The use of radioactive iodine therapy in hyperthyroidism. JAMA 1946, 131, 81–86.
6. Seidlin, S.M. Radioactive iodine therapy: Effect on functioning metastases of adenocarcinoma of the thyroid. JAMA 1946, 132, 838–847.
7. Strosberg, J.R.; Caplin, M.E.; Kunz, P.L.; Ruszniewski, P.B.; Bodei, L.; Hendifar, A.; Mittra, E.; Wolin, E.M.; Yao, J.C.; Pavel, M.E.; et al. 177Lu-Dotatate plus long-acting octreotide versus high-dose long-acting octreotide in patients with midgut neuroendocrine tumours (NETTER-1): Final overall survival and long-term safety results from an open-label, randomised, controlled, phase 3 trial. Lancet Oncol. 2021, 22, 1752–1763.
8. Khreish, F.; Ghazal, Z.; Marlowe, R.J.; Rosar, F.; Sabet, A.; Maus, S.; Linxweiler, J.; Bartholomä, M.; Ezziddin, S. 177Lu-PSMA-617 radioligand therapy of metastatic castration-resistant prostate cancer: Initial 254-patient results from a prospective registry (REALITY Study). Eur. J. Nucl. Med. Mol. Imaging 2021, in press.
9. Sartor, O.; de Bono, J.; Chi, K.N.; Fizazi, K.; Herrmann, K.; Rahbar, K.; Tagawa, S.T.; Nordquist, L.T.; Vaishampayan, N.; El-Haddad, G.; et al. Lutetium-177–PSMA-617 for metastatic castration-resistant prostate cancer. N. Engl. J. Med. 2021, 385, 1091–1103.
10. Mikolajczak, R.; Huclier-Markai, S.; Alliot, C.; Haddad, F.; Szikra, D.; Forgacs, V.; Garnuszek, P. Production of scandium radionuclides for theranostic applications: Towards standardization of quality requirements. EJNMMI Radiopharm. Chem. 2021, 6, 19.
11. Price, E.W.; Orvig, C. Matching chelators to radiometals for radiopharmaceuticals. Chem. Soc. Rev. 2014, 43, 260–290.
12. Aime, S.; Calabi, L.; Cavallotti, C.; Gianolio, E.; Giovenzana, G.B.; Losi, P.; Maiocchi, A.; Palmisano, G.; Sisti, M. : A new structural entry for an improved generation of MRI contrast agents. Inorg. Chem. 2004, 43, 7588–7590.
13. Baranyai, Z.; Uggeri, F.; Giovenzana, G.B.; Bényei, A.; Brücher, E.; Aime, S. Equilibrium and kinetic properties of the lanthanoids(III) and various divalent metal complexes of the heptadentate ligand AAZTA. Chem. Eur. J. 2009, 15, 1696–1705.
14. Mathias, C.J.; Sun, Y.; Welch, M.J.; Connett, J.M.; Philpott, G.W.; Martell, A.E. N,N′-bis(2-hydroxybenzyl)-1-(4-bromoacetamidobenzyl)-1,2-ethylene-diamine-N,N′-diacetic acid: A new bifunctional chelate for radio-labeling antibodies. Bioconjug. Chem. 1990, 1, 204–211.
15. Eder, M.; Wängler, B.; Knackmuss, S.; LeGall, F.; Little, M.; Haberkorn, M.; Mier, W.; Eisenhut, M. Tetrafluorophenolate of HBED-CC: A versatile conjugation agent for 68Ga-labeled small recombinant antibodies. Eur. J. Nucl. Med. Mol. Imaging 2008, 35, 1878–1886.
16. Hennrich, U.; Eder, M. Ga-PSMA-11: The first FDA-approved 68Ga-radiopharmaceutical for PET imaging of prostate cancer. Pharmaceuticals 2021, 14, 713.

17. Ermelindo, A.; Gambino, G.; Tei, L. Synthesis of a mixed carboxylate–phosphinate AAZTA-like ligand and relaxometric characterization of its GdIII complex. Tetrahedron Lett. 2013, 54, 6378–6380.

18. Elemento, E.M.; Parker, D.; Aime, S.; Gianolio, E.; Lattuada, L. Variation of water exchange dynamics with ligand structure and stereochemistry in lanthanide complexes based on 1,4-diazepine derivatives. Org. Biomol. Chem. 2009, 7, 1120–1131.

19. Guanci, C.; Pinalli, R.; Aime, S.; Gianolio, E.; Lattuada, L.; Giovenzana, G.B. Synthesis of phosphonic analogues of AAZTA and relaxometric evaluation of the corresponding Gd(III) complexes as potential MRI contrast agents. Tetrahedron Lett. 2015, 56, 1994–1997.

20. Camera, L.; Kinuya, S.; Garmestani, K.; Wu, C.; Brechbiel, M.W.; Pai, L.H.; McMurry, T.J.; Gansow, O.A.; Pastan, I.; Paik, C.H. Evaluation of the serum stability and in vivo biodistribution of CHX-DTPA and other ligands for yttrium labeling of monoclonal antibodies. J. Nucl. Med. 1994, 35, 882–889.

21. Stimmel, J.B.; Kull, F.C. Samarium-153 and lutetium-177 chelation properties of selected macrocyclic and acyclic ligands. Nucl. Med. Biol. 1998, 25, 117–125.

22. Vágner, A.; D'Alessandria, C.; Gambino, G.; Schwaiger, M.; Aime, S.; Maiocchi, A.; Tóth, I.; Baranyai, Z.; Tei, L. A Rigidified AAZTA-like ligand as efficient chelator for 68Ga radiopharmaceuticals. ChemistrySelect 2016, 1, 163–171.

23. Martinelli, J.; Martorana, E.; Tei, L. Synthesis of a rigidified bicyclic AAZTA-like ligand and relaxometric characterization of its GdIII complex. Tetrahedron Lett. 2020, 61, 152573.

24. Rosa, L.D.; Romanelli, A.; D'Andrea, L.D. Introduction to chemical ligation reactions. In Chemical Ligation; D'Andrea, L.D., Romanelli, A., Eds.; John Wiley & Sons, Inc.: Hoboken, NJ, USA, 2017; pp. 1–87. ISBN 978-1-119-04411-6.

25. Spang, P.; Herrmann, C.; Roesch, F. Bifunctional gallium-68 chelators: Past, present, and future. Semin. Nucl. Med. 2016, 46, 373–394.

26. Sengar, R.S.; Nigam, A.; Geib, S.J.; Wiener, E.C. Syntheses and crystal structures of gadolinium and europium complexes of AAZTA analogues. Polyhedron 2009, 28, 1525–1531.

27. Gianolio, E.; Giovenzana, G.B.; Ciampa, A.; Lanzardo, S.; Imperio, D.; Aime, S. A novel method of cellular labeling: Anchoring MR-imaging reporter particles on the outer cell surface. ChemMedChem 2008, 3, 60–62.

28. Bandoli, G.; Dolmella, A.; Tisato, F.; Porchia, M.; Refosco, F. Mononuclear six-coordinated Ga(III) complexes: A comprehensive survey. Coord. Chem. 2009, 253, 56–77.

29. Parker, D.; Waldron, B.P. Conformational analysis and synthetic approaches to polydentate perhydro-diazepine ligands for the complexation of gallium(III). Org. Biomol. Chem. 2013, 11, 2827–2838.

30. Klasen, B.; Moon, E.S.; Rösch, F. AAZTA5-Squaramide ester competing with DOTA-, DTPA- and CHX-A″-DTPA-analogues: Promising tool for 177Lu-labeling of monoclonal antibodies under mild conditions. Nucl. Med. Biol. 2021, 96, 80–93.

31. Grus, T.; Lahnif, H.; Klasen, B.; Moon, E.-S.; Greifenstein, L.; Roesch, F. Squaric acid-based radiopharmaceuticals for tumor imaging and therapy. Bioconjug. Chem. 2021, 32, 1223–1231.

32. Vologdin, N.; Rolla, G.A.; Botta, M.; Tei, L. Orthogonal synthesis of a heterodimeric ligand for the development of the GdIII–GaIII ditopic complex as a potential pH-sensitive MRI/PET probe. Org. Biomol. Chem. 2013, 11, 1683–1690.

33. Lowe, M.P.; Parker, D.; Reany, O.; Aime, S.; Botta, M.; Castellano, G.; Gianolio, E.; Pagliarin, R. pH-Dependent modulation of relaxivity and luminescence in macrocyclic gadolinium and europium complexes based on reversible intramolecular sulfonamide ligation. J. Am. Chem. Soc. 2001, 123, 7601–7609.

34. Wu, Z.; Zha, Z.; Choi, S.R.; Plössl, K.; Zhu, L.; Kung, H.F. New 68Ga-phenA bisphosphonates as potential bone imaging agents. Nucl. Med. Biol. 2016, 43, 360–371.

35. Orteca, G.; Sinnes, J.-P.; Rubagotti, S.; Iori, M.; Capponi, P.C.; Piel, M.; Rösch, F.; Ferrari, E.; Asti, M. Gallium-68 and scandium-44 labelled radiotracers based on curcumin structure linked to bifunctional chelators: Synthesis and characterization of potential PET radiotracers. J. Inorg. Biochem. 2020, 204, 110954.

36. Sinnes, J.-P.; Bauder-Wüst, U.; Schäfer, M.; Moon, E.S.; Kopka, K.; Rösch, F. 68Ga, 44Sc and 177Lu-labeled AAZTA5-PSMA-617: Synthesis, radiolabeling, stability and cell binding compared to DOTA-PSMA-617 analogues. EJNMMI Radiopharm. Chem. 2020, 5, 28.

37. Ghiani, S.; Hawala, I.; Szikra, D.; Trencsényi, G.; Baranyai, Z.; Nagy, G.; Vágner, A.; Stefania, R.; Pandey, S.; Maiocchi, A. Synthesis, radiolabeling, and pre-clinical evaluation of Sc-AAZTA conjugate PSMA inhibitor, a new tracer for high-efficiency imaging of prostate cancer. Eur. J. Nucl. Med. Mol. Imaging 2021, 48, 2351–2362.

38. Le Roux, J.; Kleynhans, J.; Rubow, S. The use of HEPES-buffer in the production of gallium-68 radiopharmaceuticals—Time to reconsider strict Pharmacopoeial limits? EJNMMI Radiopharm. Chem. 2021, 6, 15.

39. Puré, E.; Blomberg, R. Pro-tumorigenic roles of fibroblast activation protein in cancer: Back to the basics. Oncogene 20 18, 37, 4343–4357.

40. Jansen, K.; Heirbaut, L.; Verkerk, R.; Cheng, J.D.; Joossens, J.; Cos, P.; Maes, L.; Lambeir, A.-M.; De Meester, I.; Augu styns, K.; et al. Extended structure–activity relationship and pharmacokinetic investigation of (4-quinolinoyl)glycyl-2-cya nopyrrolidine inhibitors of fibroblast activation protein (FAP). J. Med. Chem. 2014, 57, 3053–3074.

41. Lindner, T.; Loktev, A.; Giesel, F.; Kratochwil, C.; Altmann, A.; Haberkorn, U. Targeting of activated fibroblasts for imagin g and therapy. EJNMMI Radiopharm. Chem. 2019, 4, 16.

42. Lindner, T.; Giesel, F.L.; Kratochwil, C.; Serfling, S.E. Radioligands targeting fibroblast activation protein (FAP). Cancer s 2021, 13, 5744.

43. Moon, E.S.; Elvas, F.; Vliegen, G.; De Lombaerde, S.; Vangestel, C.; De Bruycker, S.; Bracke, A.; Eppard, E.; Greifenst ein, L.; Klasen, B.; et al. Targeting fibroblast activation protein (FAP): Next generation PET radiotracers using squarami de coupled bifunctional DOTA and DATA5m chelators. EJNMMI Radiopharm. Chem. 2020, 5, 19.

44. Moon, E.S.; Van Rymenant, Y.; Battan, S.; De Loose, J.; Bracke, A.; Van der Veken, P.; De Meester, I.; Rösch, F. In vitr o evaluation of the squaramide-conjugated fibroblast activation protein inhibitor-based agents AAZTA5.SA.FAPi and D OTA.SA.FAPi. Molecules 2021, 26, 3482.

45. Krenning, E.P.; Breeman, W.A.P.; Kooij, P.P.M.; Lameris, J.S.; Bakker, W.H.; Koper, J.W.; Ausema, L.; Reubi, J.C.; Lam berts, S.W.J. Localisation of endocrine-related tumours with radioiodinated analogue of somatostatin. Lancet 1989, 33 3, 242–244.

46. Bakker, W.H.; Albert, R.; Bruns, C.; Breeman, W.A.P.; Hofland, L.J.; Marbach, P.; Pless, J.; Pralet, D.; Stolz, B.; Koper, J.W.; et al. -Octreotide, a potential radiopharmaceutical for imaging of somatostatin receptor-positive tumors: Synthesi s, radiolabeling and In vitro validation. Life Sci. 1991, 49, 1583–1591.

47. Otte, A.; Jermann, E.; Behe, M.; Goetze, M.; Bucher, H.C.; Roser, H.W.; Heppeler, A.; Mueller-Brand, J.; Maecke, H.R. DOTATOC: A powerful new tool for receptor-mediated radionuclide therapy. Eur. J. Nucl. Med. 1997, 24, 792–795.

48. Reubi, J.C.; Schär, J.C.; Waser, B.; Wenger, S.; Heppeler, A.; Schmitt, J.S.; Mäcke, H.R. Affinity profiles for human som atostatin receptor subtypes SST1-SST5 of somatostatin radiotracers selected for scintigraphic and radiotherapeutic us e. Eur. J. Nucl. Med. 2000, 27, 273–282.

49. Wild, D.; Schmitt, J.S.; Ginj, M.; Mäcke, H.R.; Bernard, B.F.; Krenning, E.; de Jong, M.; Wenger, S.; Reubi, J.-C. DOTA- NOC, a high-affinity ligand of somatostatin receptor subtypes 2, 3 and 5 for labelling with various radiometals. Eur. J. N ucl. Med. Mol. Imaging 2003, 30, 1338–1347.

50. Manzoni, L.; Belvisi, L.; Arosio, D.; Bartolomeo, M.P.; Bianchi, A.; Brioschi, C.; Buonsanti, F.; Cabella, C.; Casagrande, C.; Civera, M.; et al. Synthesis of Gd and 68Ga complexes in conjugation with a conformationally optimized RGD sequ ence as potential MRI and PET tumor-imaging probes. ChemMedChem 2012, 7, 1084–1093.

51. Reubi, J.C. Targeting CCK receptors in human cancers. Curr. Top. Med. Chem. 2007, 7, 1239–1242.

52. Reubi, J.C.; Waser, B. Concomitant expression of several peptide receptors in neuroendocrine tumours: Molecular basi s for in vivo multireceptor tumour targeting. Eur. J. Nucl. Med. Mol. Imaging 2003, 30, 781–793.

53. Klingler, M.; Hörmann, A.A.; Guggenberg, E.V. Cholecystokinin-2 receptor targeting with radiolabeled peptides: Current status and future directions. Curr. Med. Chem. 2020, 27, 7112–7132.

54. Pfister, J.; Summer, D.; Rangger, C.; Petrik, M.; von Guggenberg, E.; Minazzi, P.; Giovenzana, G.B.; Aloj, L.; Decristofo ro, C. Influence of a novel, versatile bifunctional chelator on theranostic properties of a minigastrin analogue. EJNMMI Res. 2015, 5, 74.

55. Eychenne, R.; Bouvry, C.; Bourgeois, M.; Loyer, P.; Benoist, E.; Lepareur, N. Overview of radiolabeled somatostatin an alogs for cancer imaging and therapy. Molecules 2020, 25, 4012.

56. Bombardieri, E.; Ambrosini, V.; Aktolun, C.; Baum, R.P.; Bishof-Delaloye, A.; Del Vecchio, S.; Maffioli, L.; Mortelmans, L.; Oyen, W.; Pepe, G.; et al. 111In-Pentetreotide scintigraphy: Procedure guidelines for tumour imaging. Eur. J. Nucl. Med. Mol. Imaging 2010, 37, 1441–1448.

57. Sinnes, J.-P.; Nagel, J.; Rösch, F. AAZTA5/AAZTA5-TOC: Synthesis and radiochemical evaluation with 68Ga, 44Sc an d 177Lu. EJNMMI Radiopharm. Chem. 2019, 4, 18.

58. Seemann, J.; Waldron, B.; Parker, D.; Roesch, F. DATATOC: A novel conjugate for kit-type 68Ga labelling of TOC at am bient temperature. EJNMMI Radiopharm. Chem. 2016, 1, 4.

59. Giovenzana, G.B.; Palmisano, G.; Sisti, M.; Cavallotti, C.; Aime, S.; Calabi, L. Multidentate Aza Ligands Able to Comple x Metal Ions and the Use Thereof in Diagnostics and Therapy. International Patent Application No. WO2003008390A1, 30 January 2003.